

**UNCLASSIFIED**



NAVAL AIR WARFARE CENTER AIRCRAFT DIVISION  
PATUXENT RIVER, MARYLAND

# **TECHNICAL INFORMATION MEMORANDUM**



REPORT NO. NAWCADPAX/TIM-2015/282

## **SPECTRUM FATIGUE OF 7075-T651 ALUMINUM ALLOY UNDER OVERLOADING AND UNDERLOADING**

by

**E. U. Lee  
R. E. Taylor  
B. Pregger**

**15 March 2016**

Approved for public release; distribution is unlimited.

**UNCLASSIFIED**

DEPARTMENT OF THE NAVY  
NAVAL AIR WARFARE CENTER AIRCRAFT DIVISION  
PATUXENT RIVER, MARYLAND

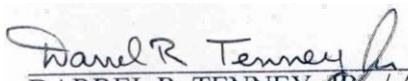
NAWCADPAX/TIM-2015/282  
15 March 2016

SPECTRUM FATIGUE OF 7075-T651 ALUMINUM ALLOY  
UNDER OVERLOADING AND UNDERLOADING

by

E. U. Lee  
R. E. Taylor  
B. Pregger

**RELEASED BY:**

 3/15/2016  
\_\_\_\_\_  
DARREL R. TENNEY, JR. / AIR-4.3.4 / DATE  
Head, Materials Engineering Division  
Naval Air Warfare Center Aircraft Division

REPORT DOCUMENTATION PAGE			Form Approved OMB No. 0704-0188		
Public reporting burden for this collection of information is estimated to average 1 hour per response, including the time for reviewing instructions, searching existing data sources, gathering and maintaining the data needed, and completing and reviewing this collection of information. Send comments regarding this burden estimate or any other aspect of this collection of information, including suggestions for reducing this burden, to Department of Defense, Washington Headquarters Services, Directorate for Information Operations and Reports (0704-0188), 1215 Jefferson Davis Highway, Suite 1204, Arlington, VA 22202-4302. Respondents should be aware that notwithstanding any other provision of law, no person shall be subject to any penalty for failing to comply with a collection of information if it does not display a currently valid OMB control number. <b>PLEASE DO NOT RETURN YOUR FORM TO THE ABOVE ADDRESS.</b>					
1. REPORT DATE 15 March 2016		2. REPORT TYPE Technical Information Memorandum		3. DATES COVERED 2015	
4. TITLE AND SUBTITLE  Spectrum Fatigue of 7075-T651 Aluminum Alloy under Overloading and Underloading			5a. CONTRACT NUMBER		
			5b. GRANT NUMBER		
			5c. PROGRAM ELEMENT NUMBER		
6. AUTHOR(S)  E. U. Lee R. E. Taylor B. Pregger			5d. PROJECT NUMBER		
			5e. TASK NUMBER		
			5f. WORK UNIT NUMBER		
7. PERFORMING ORGANIZATION NAME(S) AND ADDRESS(ES)  Naval Air Warfare Center Aircraft Division Code 4341, Bldg. 2188 22347 Cedar Point Road, Patuxent River, MD 20670			8. PERFORMING ORGANIZATION REPORT NUMBER  NAWCADPAX/TIM-2015/282		
9. SPONSORING/MONITORING AGENCY NAME(S) AND ADDRESS(ES)  Office of Naval Research Code 351 875 North Randolph Street Arlington, VA 22203-1995			10. SPONSOR/MONITOR'S ACRONYM(S)		
			11. SPONSOR/MONITOR'S REPORT NUMBER(S)		
12. DISTRIBUTION/AVAILABILITY STATEMENT  Approved for public release, distribution is unlimited.					
13. SUPPLEMENTARY NOTES  .					
14. ABSTRACT  A study was conducted to clarify the effects of overload, underload, stress ratio, and environment on fatigue crack growth. Fatigue crack growth tests were conducted with a 7075-T651 aluminum alloy under constant amplitude, and over- and under-loading of two different stress ratios, 0.1 and 0.85, in vacuum, air and 1 percent NaCl solution. Under constant amplitude loading, da/dN of R=0.1 and 0.85 was mostly greatest in 1 percent NaCl solution, intermediate in air and lowest in vacuum, and it was greater at R=0.85 than at R=0.1. Furthermore, the da/dN under constant amplitude loading was similar to that of underloading at high $\Delta K$ . On the other hand, da/dN was greater under underloading than under overloading, greater in 1 percent NaCl solution, and greater at R=0.85 than at R=0.1.  To account for the load spectrum sequence effects, the recently developed cycle-by-cycle fatigue crack growth (FCG) model, UniGrow, was chosen in this study. This model regards the FCG as a process of successive crack re-initiation in the crack tip region, controlled by a two-parameter driving force. Employing the UniGrow equation, the variation of crack length with number of loading cycle was predicted. The prediction and the fatigue test life were found to agree fairly closely.					
15. SUBJECT TERMS  Spectrum Fatigue, Overloadng, Underloading, Stress Ratio, Environment, Fatigue Crack Growth, Loading Cycle					
16. SECURITY CLASSIFICATION OF:			17. LIMITATION OF ABSTRACT	18. NUMBER OF PAGES	19a. NAME OF RESPONSIBLE PERSON E. U. Lee
a. REPORT	b. ABSTRACT	c. THIS PAGE			19b. TELEPHONE NUMBER (include area code)
Unclassified	Unclassified	Unclassified			301-342-8069

## SUMMARY

Fatigue tests of 7075-T651 aluminum alloy were conducted under constant amplitude loading, and spectrum loadings of overload and underload in vacuum of  $4 \times 10^{-8}$  torr, laboratory air of relative humidity about 50 percent and aqueous 1 percent NaCl solution of pH 2 at ambient temperature. The loading frequency was about 5 Hz, the growing crack length was measured, using direct current potential drop technique, and the fatigue crack growth rate was determined. The recently developed cycle-by-cycle fatigue crack growth (FCG) model, UniGrow, was studied to find out whether this model is applicable for the clarification of the load spectrum sequence effect. Employing the UniGrow equation, the variation of crack length with number of loading cycle was predicted. The prediction and the fatigue test life were compared and evaluated.

## Contents

	<u>Page No.</u>
Introduction.....	1
Background .....	1
Purpose.....	2
Methods	
Speciman.....	3
Fatigue Tests .....	3
Constant Amplitude Type .....	3
Overload Type .....	3
Underload Type .....	3
Fractography .....	3
Experimental Results .....	5
Constant Amplitude Loading Fatigue .....	5
Overloading and Underloading Fatigue.....	5
Fatigue Crack Length.....	5
Fatigue Crack Growth Rate .....	6
Fractograph .....	7
Discussion .....	9
Crack Growth Retardation and Acceleration .....	9
UniGrow Model .....	9
Comparison of Test Result and UniGrow Prediction .....	9
Conclusions .....	11
References .....	13
Appendix	
A. Figures.....	15
Distribution .....	25

## ACKNOWLEDGEMENTS

The support for this study from the Office of Naval Research under Contract N0001415WX00141 is gratefully acknowledged. Furthermore, the authors appreciate Mr. William Nickerson of ONR for his kind guidance and interest.

## INTRODUCTION

Most structural members and machine components are subjected in service to cyclic loadings of varying amplitude. The variation in stress level follows either a regular or random pattern. The resulting crack growth is affected by the applied load sequence in the early stage (crack initiation) and in the later stage (crack propagation) of fatigue. The fatigue crack growth is known to be retarded by tensile overloads and accelerated by compressive overloads (underloads). However, the phenomenon and mechanism of the load sequence effects, especially those of overloading and underloading, on fatigue crack growth in different environments remain to be clarified.

## BACKGROUND

Structural components are mostly subjected to variable amplitude or spectrum fatigue loading in various service environments. Blades in gas turbine engines experience low-amplitude, high-frequency vibration during operation, superimposed on a relatively smaller number of cycles of fatigue loading due to start-up and shut-down. Railway tracks are subjected to random loading depending on the frequency and loading conditions associated with the passage of trains. The rotors and bearings of a turbo-generator are subjected to an overload (OL) during every start-up. On the ground, the lower wing skin of the aircraft is under compression. During flight, variable loads due to gust are superimposed on a mean tensile load corresponding to an undisturbed flight. The transition from a compressive load on the ground to a tensile load during flight is an important load cycle in itself and is usually referred to as a ground-air-ground cycle.

The fatigue crack growth under spectrum loading is affected by load interaction, such as crack growth acceleration, retardation or even arrest (1, 2). Due to the load interaction effects, reliability, and life assessment of structural components entails considerable difficulties under spectrum loading. For instance, high OL peaks cause retardation effects whereas underload (UL) peaks accelerate the crack growth and weaken the preceding retardation effect (3-6).

To account for the load spectrum effects, cycle-by-cycle fatigue crack growth prediction models were developed. They are divided into three main groups, Willenborg (3), Wheeler (4), and UniGrow (7, 8) ones. The first and second ones consider that the current cyclic crack tip plastic zone develops inside a larger zone created by the preceding OL. Furthermore, the second one is based on crack closure, and includes plasticity-induced crack closure model (9) and strip yield model (10). Third group, the unified two parameter model is based on the elastic-plastic crack tip stress-strain history (7, 8).

In addition, the fatigue crack growth is also influenced strongly by environments. It is well established that seawater and other aggressive environments accelerate fatigue crack growth (11, 12). However, other investigators (13-18) reported that aggressive environments could cause fatigue crack growth retardation or even arrest.

Creager and Paris (19) showed that crack blunting can decrease the stress intensity factor and hence cause crack growth retardation. Bristoll, and Roeleveld, (14) and Johnson et al (15)

proposed that this could account for fatigue crack growth arrest in structural steel during fatigue at 0.1 Hz under tidal immersion conditions. So did Radon et al for crack stoppage in mild steel at 0.25 Hz in 3.5 percent NaCl solution and Atkinson and Lindley (20) for A533 steel fatigued in distilled water at 90°C. Crack branching will also decrease the stress intensity factor, as shown by Vitek (21). Tu and Seth (17) used this argument to account for the increase in threshold  $\Delta K$  level for turbine rotor steels when fatigued in steam instead of air. Another mechanism for crack retardation is corrosion product wedging, which increases the minimum K and hence reduce the stress intensity range  $\Delta K$ . Nordmark and Fricke (18) produced strong evidence that this was the reason for crack arrest of 7475-T351 aluminum alloy fatigued in artificial sump water. They showed that minimum crack-opening displacement, which can be directly related to K, increased when fatigue crack growth arrest occurred. Another result (13) showed crack retardation and stoppage in two structural steels during constant amplitude fatigue at 10 Hz frequency in oxygen-saturated seawater.

## PURPOSE

This study is initiated to clarify the fatigue crack growth behavior of a 7075-T651 aluminum alloy under spectrum loading with periodic OL or UL cycles in different environments. Furthermore, the possible mechanisms, synergistic effects and implications are considered.



## METHODS

### SPECIMEN

Middle-tension M(T) specimen was machined in L-T orientation from a 7075-T651 aluminum alloy extrusion of 127x127x394 mm (5x5x15.5 in.). It was 102 mm (4 in.) wide, 235 mm (9.3 in.) long and 2 mm (0.086 in.) thick, and its center notch was 3 mm (1/8 in.) long. Its mechanical properties were UTS 538 MPa (78 ksi), YS 446 MPa (65 ksi) and elongation 11 percent.

### FATIGUE TESTS

The fatigue tests were conducted under constant amplitude loading and spectrum loading with periodic OL or UL cycles at ambient temperature in an MTS machine, Figure A-1. The loading frequency was 5 Hz, the growing crack length  $2a$  was measured, employing direct current potential drop technique, and the fatigue crack growth rate  $da/dN$  was computed. Subsequently, half crack length vs. number of loading cycle  $a$  vs.  $N$  and fatigue crack growth rate vs. stress intensity range  $da/dN$  vs.  $\Delta K$  were plotted. The main features of the loadings were:

#### CONSTANT AMPLITUDE TYPE

Constant Amplitude Loading of Stress Ratio  $R=0.1$  or  $0.85$  in Vacuum of  $4 \times 10^{-8}$  Torr , Air and 1 percent NaCl Solution of pH 2

#### OVERLOAD TYPE

A 100 percent OL-Spike at Every 10,000 Cycles of  $R=0.1$  or  $0.8$  in Vacuum of  $4 \times 10^{-8}$  Torr and 1 percent NaCl Solution of pH 2, Figure A-2

#### UNDERLOAD TYPE

A 100 percent UL-Spike at Every 10,000 Cycles of  $R=0.1$  or  $0.85$  in Vacuum of  $4 \times 10^{-8}$  Torr and 1 percent NaCl Solution of pH 2, Figure A-2

### FRACTOGRAPHY

After the fatigue test, the morphology of the specimen fracture surface was examined with a JEOL JSM-6460LV scanning electron microscope, operated at an acceleration voltage of 20 kV.

THIS PAGE INTENTIONALLY LEFT BLANK

## EXPERIMENTAL RESULTS

### CONSTANT AMPLITUDE LOADING FATIGUE

Figure A-3 shows the effect of environment on fatigue crack growth under constant amplitude loading at two different stress ratios 0.1 and 0.85. Each of the two sets of fatigue crack growth rate vs stress intensity range ( $da/dN$  vs  $\Delta K$ ) curves for  $R=0.1$  and 0.85 consists of three curves for three different test environments, vacuum (dark), air (red) and 1 percent NaCl solution (yellow).

In the case of  $R=0.1$ , at lower  $\Delta K$ , the  $da/dN$  is greatest in air, intermediate in NaCl solution and lowest in vacuum. The slower fatigue crack growth in NaCl solution than in air is attributable to corrosion product-induced crack closure. At intermediate  $\Delta K$ ,  $da/dN$  is similar in air and NaCl solution, and it is lowest in vacuum. At high  $\Delta K$ , the three curves tend to converge together and the fatigue crack growth rates are similar in the three environments.

In the case of  $R=0.85$ , at low and intermediate  $\Delta K$ , the  $da/dN$  is slightly greater in NaCl solution, intermediate in air and lowest in vacuum. This evidences that the corrosion product-induced crack closure is absent at  $R=0.85$ . At high  $\Delta K$ , the three curves converge together and the fatigue crack growth rates become similar in the three environments.

Figure A-4 shows the effect of  $R$  on  $da/dN$  and the threshold stress intensity range for fatigue crack growth  $\Delta K_{th}$  in the three environments. The red curve indicates the result of test at  $R=0.85$  and the dark one that at  $R=0.1$ . The  $da/dN$  is greater and the  $\Delta K_{th}$  is smaller at  $R=0.85$  than at  $R=0.1$  in all of the three environments.

### OVERLOADING AND UNDERLOADING FATIGUE

#### FATIGUE CRACK LENGTH

Figure A-5 shows the variation of half crack length with number of loading cycle  $N$  during OL and UL spectrum loading at  $R=0.1$  in vacuum and 1 percent NaCl solution. The crack growth is faster and the fatigue life is shorter under the UL spectrum loading than the OL one in both of the environments, Figures A-5(a) and (b).

Figure A-6 shows the effect of environment on the variation of half crack length with number of loading cycle under OL and UL spectrum loading at  $R=0.1$ . The crack growth is faster in 1 percent NaCl solution than in vacuum under OL spectrum loading, Figure A-6(a), whereas they are similar in the two environments under UL spectrum loading, Figure A-6(b).

Figure A-7 shows the effect of spectrum loading on the variation of half crack length with number of loading cycle at  $R=0.85$  in vacuum and 1 percent NaCl solution. The crack growth under UL spectrum loading is slightly faster and the fatigue life is slightly shorter than under OL one, Figure A-7(a). On the other hand, the crack growth is much faster and the fatigue life is

much shorter under UL spectrum loading than under OL one in 1 percent NaCl solution, Figure A-7(b).

Figure A-8 shows the effect of environment on the variation of half crack length with number of loading cycle at  $R=0.85$  in vacuum and 1 percent NaCl solution. The crack growth is faster and the fatigue life is shorter in 1 percent NaCl solution than in vacuum under both of the OL and UL spectrum loadings, Figure A-8(a) and (b).

## FATIGUE CRACK GROWTH RATE

Figure A-9 shows the effect of loading on fatigue crack growth rate  $da/dN$  at  $R=0.1$  in vacuum and 1 percent NaCl solution. Yellow curve indicates constant amplitude loading, red one overloading, and dark one underloading. From these two sets of curve, it is clear that:

- In vacuum, the  $da/dN$  is greater for underloading than for constant amplitude loading at lower  $\Delta K$ , but it is similar at higher  $\Delta K$ . That is, the fatigue crack growth is accelerated by underloading at lower  $\Delta K$  in vacuum.
- In 1 percent NaCl solution, the  $da/dN$  is similar for constant amplitude loading and underloading within the range of  $\Delta K$  employed.
- Compared to the  $da/dN$  under constant amplitude loading and underloading, the  $da/dN$  under overloading is lower in vacuum and 1 percent NaCl solution. This observation indicates that the fatigue crack growth is retarded by overloading in both environments.

Figure A-10 shows the effect of environment on fatigue crack growth rate under overloading and underloading at  $R=0.1$ . Red curve indicates the test data in 1 percent NaCl solution and dark one that in vacuum. From these plots, it is clear that the fatigue crack growth is faster in 1 percent NaCl solution than in vacuum under overloading and underloading, Figures 10(a) and (b).

Figure A-11 shows the effect of loading on fatigue crack growth rate at  $R=0.85$  in 1 percent NaCl solution. Yellow curve indicates the constant amplitude loading data, red one the overloading data and dark one the underloading data. From these plots, it is clear that:

- The  $da/dN$  is mostly similar for constant amplitude loading and underloading and
- The  $da/dN$  is lowest for overloading, indicating retardation of fatigue crack growth by overloading.

Figure A-12 shows the effect of environment on fatigue crack growth rate under overloading at  $R=0.85$ . Red curve indicates the result of test in 1 percent NaCl solution, and dark one that in vacuum. From this plot, it is clear that the  $da/dN$  is greater in 1 percent NaCl solution than in vacuum for overloading.

## FRACTOGRAPH

Typical fractographs of those specimens, subjected to OL and UL spectrum fatigue loading at  $R=0.1$  in vacuum, are shown in Figures A-13 and -14. The optical fractograph of the OL spectrum fatigue tested specimen shows beach-marks, Figure 13(a), whereas that of UL spectrum fatigue tested shows quite faint ones, Figure A-13(b). The SEM fractograph of the OL spectrum fatigue tested specimen shows fatigue striations clearly, Figure A-14(a), whereas that of UL spectrum fatigue tested specimen faint ones, Figure A-14(b).

The spacing of the fatigue striation is measured to be increasing with increasing crack length, initially steeply and then moderately, as shown in Figure A-15.

THIS PAGE INTENTIONALLY LEFT BLANK

## DISCUSSION

### CRACK GROWTH RETARDATION AND ACCELERATION

As observed in this study, other investigators also observed crack growth retardation and acceleration during variable amplitude fatigue loading. For example, on application of a single peak OL, the crack first accelerates [22, 23], and this is followed by a prolonged period of decelerated crack growth. On the other hand, after a single compressive UL, a brief acceleration of the crack growth is observable. However, the subsequent crack growth is comparable to that of a single peak tensile OL.

Several mechanisms have been proposed to account for the crack growth retardation following a single OL. Some of them include: (i) crack tip blunting [19]; (ii) deflection or bifurcation of the crack [24]; (iii) residual compressive stresses ahead of the crack tip [3, 4], and (iv) plasticity-induced crack closure in the wake of the crack tip [25, 26]. However, in this study, any crack deflection or bifurcation has not been detected during overloading. After a single compressive underloading, tensile residual stress is generated behind the crack tip. The tensile stress results in higher crack tip driving force for crack growth and an instantaneous acceleration of crack growth [27].

### UNIGROW MODEL

The UniGrow model is based on the elastic-plastic crack tip stress-strain history. This model regards the FCG as a process of successive crack re-initiation in the crack tip region, controlled by a two-parameter ( $K_{\max}$  and  $\Delta K$ ) driving force. The basic equation of this model is  $da/dN = C[(K_{\max, \text{tot}})^p (\Delta K_{\text{tot}})^{(1-p)}]^\gamma = C[\Delta \kappa]^\gamma$ ,  $a = \int C[\Delta \kappa]^\gamma dN$

where

$$C = 2\rho^*[(\psi_{y,1})^2/2^{(n'+3)/(n'+1)}\sigma'_f\epsilon'_f\pi E\rho^*]^{-\{1/(b+c)\}}, \quad p = n'/(n' + 1), \quad \gamma = -2/(b + c)$$

a: half crack length, b: fatigue strength exponent, c: fatigue ductility exponent, C: fatigue crack growth constant,  $K_{\max, \text{tot}}$ =total maximum stress intensity factor,  $n'$ : cyclic strain hardening exponent, p: driving force constant,  $\epsilon'_f$ : fatigue ductility coefficient,  $\gamma$ : fatigue crack growth equation exponent,  $\rho^*$ : notch tip radius or elementary material block size,  $\sigma'_f$ : fatigue strength coefficient,  $\psi_i$ : average constant corresponding to  $i$ th elementary block.

### COMPARISON OF TEST RESULT AND UNIGROW PREDICTION

Figures A-16 and A-17 compare the test result, Figure A-5, and the corresponding UniGrow prediction for the variation of crack length vs number of loading cycle under OL and UL spectrum loading in vacuum and 1 percent NaCl solution, respectively.

In vacuum, the prediction life is quite shorter than the test life under OL spectrum loading, whereas the test data and prediction are close under UL spectrum loading, Figure A-16. This

comparison indicates that the UniGrow model accounts for the FCG retardation by tensile OL too little in vacuum.

In 1 percent NaCl solution, the prediction life is shorter than the test life under OL spectrum loading, whereas the test data and prediction are in good agreement under UL spectrum loading, Figure A-17.



## CONCLUSIONS

Under constant amplitude loading, overloading and underloading, fatigue crack growth rate is greater at stress ratio 0.85 than at 0.1.

1 percent NaCl solution accelerates but vacuum retards the fatigue crack growth.

OL retards but the UL accelerates the fatigue crack growth in vacuum and 1 percent NaCl solution.

The UniGrow model provides close estimate of fatigue crack growth (FCG) for underloading, but conservative one for overloading in vacuum and 1 percent NaCl solution. This evidences that the UniGrow model accounts for the FCG acceleration by underloading correctly, but it does not for the FCG retardation by overloading.

THIS PAGE INTENTIONALLY LEFT BLANK

## REFERENCES

1. R. J. H. Wanhill and J. Schijve: in *Fatigue Crack Growth Under Variable Amplitude Loading*, J. Petit, et al. Eds. Elsevier Applied Science Publishers, London, 1988, p. 326.
2. N. Ranganathan, et al., ASTM STP 1049, ASTM, Philadelphia, 1989, p. 374.
3. S. Wilenborg, R. M. Eagle, and H. A. Wood: *A Crack Growth Retardation Model Using An Effective Stress Concept*. AFFDL-TM-FBR-81-1, Air Force Dynamics Laboratory, 1971.
4. O. Wheeler: *J Basic Eng* 1972, vol 94D, p. 181.
5. C. Bathias, and M. Vancon: *Eng Fracture Mech*, 1978, vol 10, pp. 409-24.
6. P. E. Bretz PE, A. K. Vasudevan, R. J. Bucci, and R. C. Malcolm: in *Fatigue Crack Growth Behavior of 7xxx Aluminum Alloys Under Simple Variable Amplitude Loading*, *Fracture Mechanics Fifteenth Symposium*, ASTM STP 833, 1984, pp. 242-65.
7. A. K. Vasudevan , K. Sadananda K and G. Glinka: *Int J Fatigue*, 2001, vol 23, pp. S39-53.
8. A. H. Noroozi, G. Glinka G, and S. A. Lambert: *Int J Fatigue*, 2005, vol 27, pp. 1277-96.
9. W. Elber: *Eng fract Mech*, 1970, vol 2, pp. 37-45.
10. D. S. Dougdale: *J Mech Phys Solids*, 1960, vol 8, pp. 100-8.
11. P. Shahinian and K. Sadanada: *Environmental Effects on Fatigue Behavior of Metals*, NRL Memorandum Report 4495, Naval Research Laboratory, Washington, DC, April 9, 1981.
12. C. E. Jaske, D. Brock, J. E. Slater, and W. E. Anderson: in *Corrosion Fatigue Technology*, ASTM STP 642, ASTM, 1978, pp. 19-47.
13. J. H. Veen, J. Wekken, and J. L. Ewalds: *Report*, Delft University of Technology, Dept. of Metallurgy, Delft, The Nethermands, Oct 1978.
14. P. Bristol, and J. A. Roeleveld: in *Proceedings, European Offshore Steels Research Seminar*, The Welding Institute, Abbingdon Hall, Abbingdon, Cambridge, U. K., 1980, pp. VI/p. 18-1-VI/p. 18-10.
15. R. Johnson, L. Bretherton, B. Tomkins, P. M. Scott, and D. R. V. Silverster: in *Proceedings, European Offshore Steels Research Seminar*, The Welding Institute, Abbingdon Hall, Abbingdon, Cambridge, U. K., 1980, pp. VI/p. 15-VI/p. 15-15.
16. J. C. Radon, C. M. Branco, and L. E. Culver: *Int J Fracture Mech*, 1976, vol 12, pp. 467-469.

17. L. K. L. Tu and B. B. Seth, J Test Eva, 1978, vol 6, No. 5, pp. 301-03.
18. G. E. Nordmark and W. G. Fricke: J. Test Eva, 1978, vol 6, No. 1, pp. 55-74.
19. M. Creager and P. C. Paris: I J Fract Mech, 1967, vol 3, pp. 247-52.
20. J. D. Atkinson and T. C. Lindley: in The Influence of Environment on Fatigue, Proceedings of IME-Conference, London, 1977.
21. V. Vitek: I J Fract Mech, 1977, vol. 13, pp. 481-501.
22. D. M. Corby and P. F. Packman: Eng. Fract. Mech, 1973, pp. 479-97.
23. J. Lankford and D. L. Davidson: in Advances in Fracture Research, Proceedings, Fifth International Conference on Fracture, D. Francois et al, Eds., Pergamon Press, 1981, pp. 899-906.
24. S. Suresh: Eng. Fract. Mech., 1983, vol 18, pp. 577-93.
25. G. H. Bray, A. P. Reynolds and E. A. Starke, Jr., Met Trans A, 1992, vol. 22A, pp. 3055-66.
26. W. Elber: ASTM STP 486, 1971, pp. 230-42.
27. S. Y. Lee, H. Choo, P. K. Liaw, R. B. Rogge and M. A. Ghargghouri: Effect of Overload and Underload on Residual Stress, Crack Plasticity, and the Crack Growth Rate, Experimental Report – Materials Science and Engineering, NRC-CNRC Annual Report 2007.

## APPENDIX A FIGURES

<u>Figure</u>	<u>Title</u>	<u>Page No.</u>
A-1	Test Set-Up in MTS Machine .....	14
A-2	Overload and Underload Spectrums .....	14
A-3	Effect of Environment on $da/dN$ under Constant Amplitude Loading .....	15
	at $R=0.1$ and $0.85$	
A-4	Effect of $R$ on $da/dN$ under Constant Amplitude Loading in Vacuum, Air, and .....	15
	1 Percent NaCl Solution	
A-5	Variation of Half Crack Length with Number of Loading Cycle at $R=0$ . ....	16
	in Vacuum and a 1 Percent NaCl Solution Under Overloading and Underloading	
A-6	Variation of Half Crack Length with Number of Loading Cycle at $R=0.1$ .....	16
	under Overloading and Underloading in Vacuum and 1 Percent NaCl Solution	
A-7	Variation of Half Crack Length with Number of Loading Cycle at $R=0.85$ .....	17
	in Vacuum and 1 Percent NaCl Solution under Overloading and Underloading	
A-8	Variation of Half Crack Length with Number of Loading Cycle under.....	17
	Overloading and Underloading in Vacuum and 1 Percent NaCl Solution	
A-9	Effect of Loading on Fatigue Crack Growth Rate at $R=0.1$ in Vacuum .....	18
	and 1 Percent NaCl Solution	
A-10	Effect of Environment on Fatigue Crack Growth Rate at $R=0.1$ under .....	18
	Overloading and Underloading	
A-11	Effect of Loading on Fatigue Crack Growth Rate at $R=0.85$ in .....	19
	1 Percent NaCl Solution	
A-12	Effect of Environment on Fatigue Crack Growth Rate at $R=0.85$ .....	19
	Under Overloading	
A-13	Optical Fractographs .....	20
A-14	SEM Fractographs .....	20
A-15	Variation of Striation Spacing with Crack Length .....	21
A-16	Graphic Comparison of Test Data and UniGrow Model Prediction for Overload.....	21
	and Underload Spectrums in Vacuum	
A-17	Graphic Comparison of Test Data and UniGrow Model Prediction for Overload .....	22
	and Underload Spectrums in 1 Percent NaCl Solution	



Figure A-1: Test Set-Up in MTS Machine

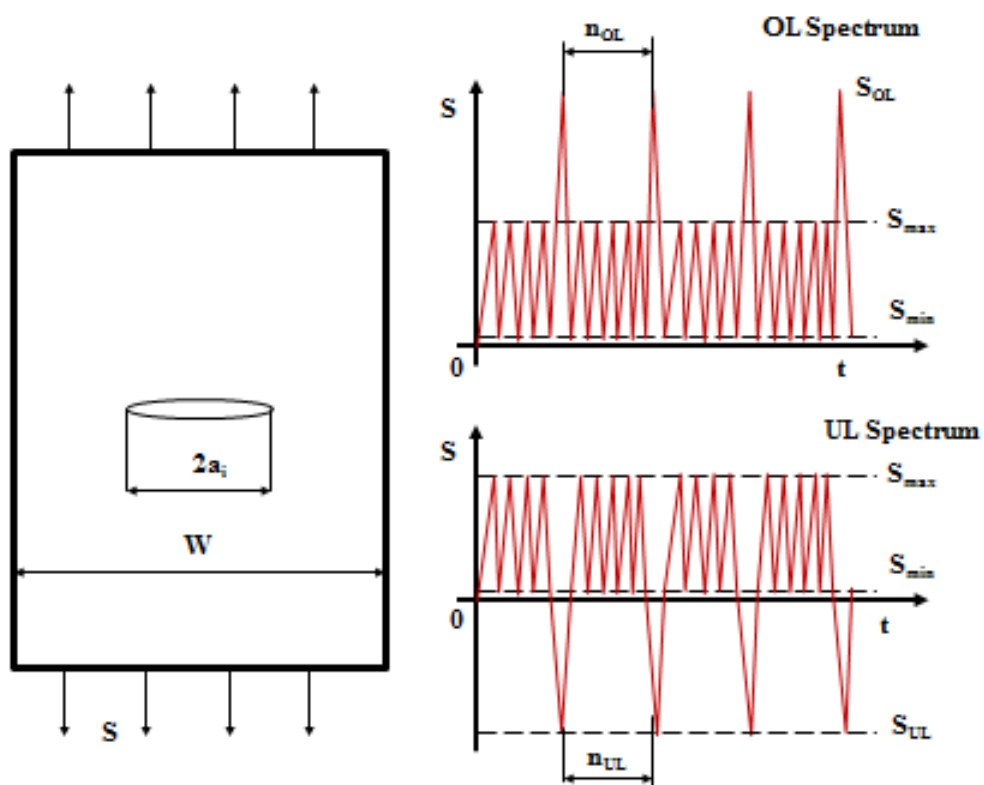


Figure A-2: Overload and Underload Spectrums

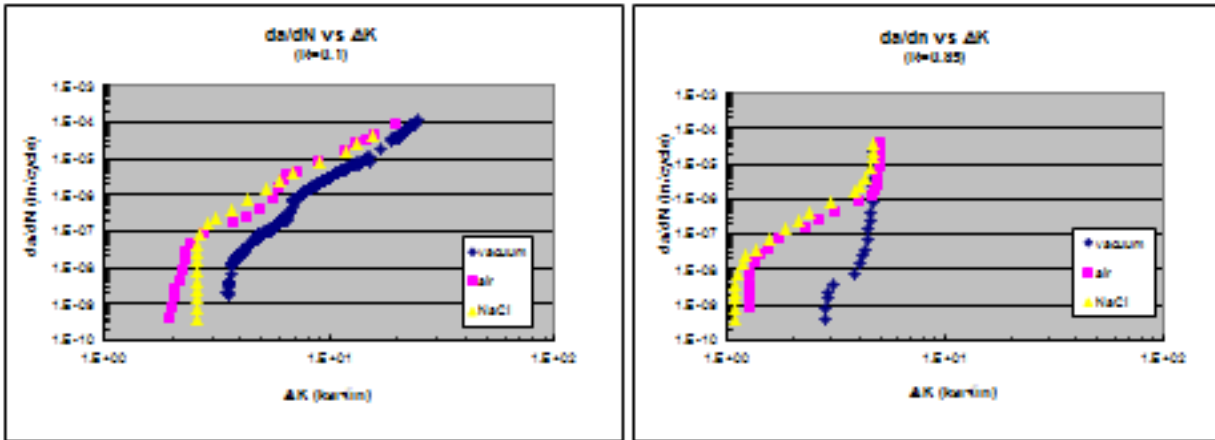


Figure A-3: Effect of Environment on  $da/dN$  under Constant Amplitude Loading at  $R=0.1$  and  $0.85$

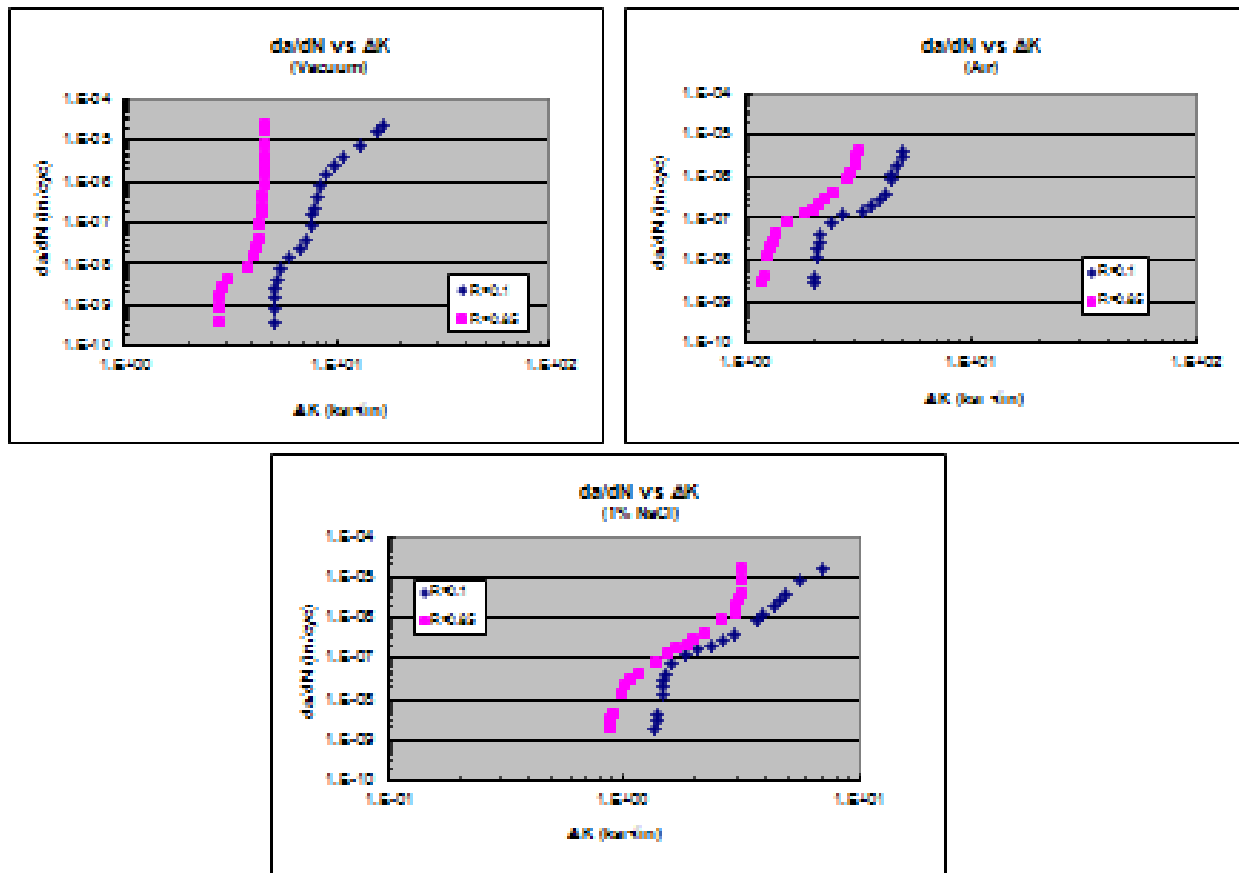


Figure A-4: Effect of  $R$  on  $da/dN$  under Constant Amplitude Loading in Vacuum, Air, and 1 Percent NaCl Solution

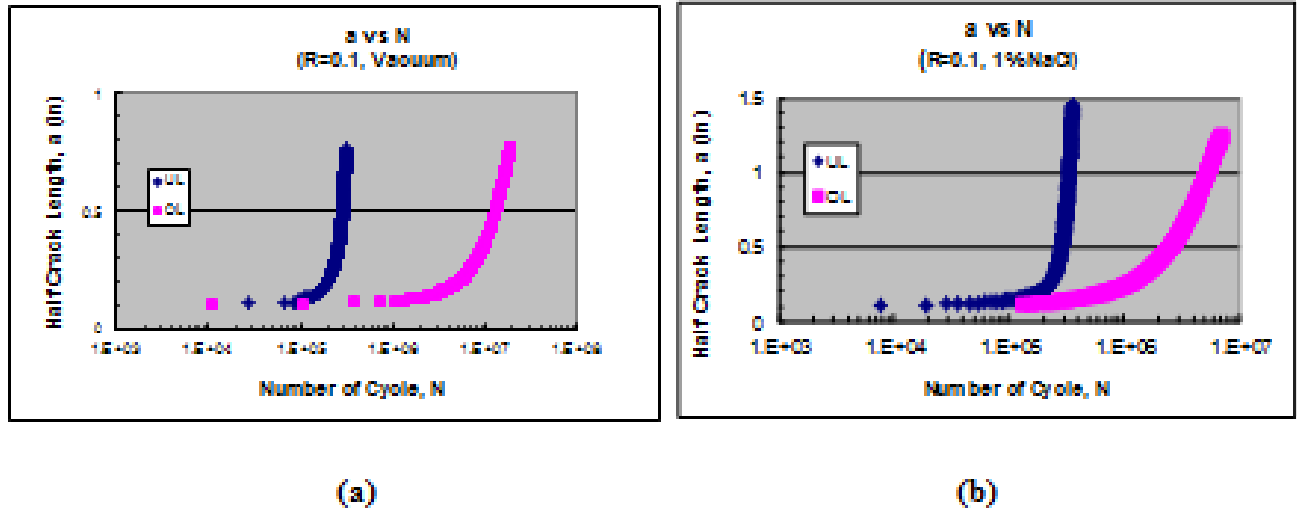


Figure A-5: Variation of Half Crack Length with Number of Loading Cycle at  $R=0.1$  in a Vacuum and 1 Percent NaCl Solution under Overloading and Underloading

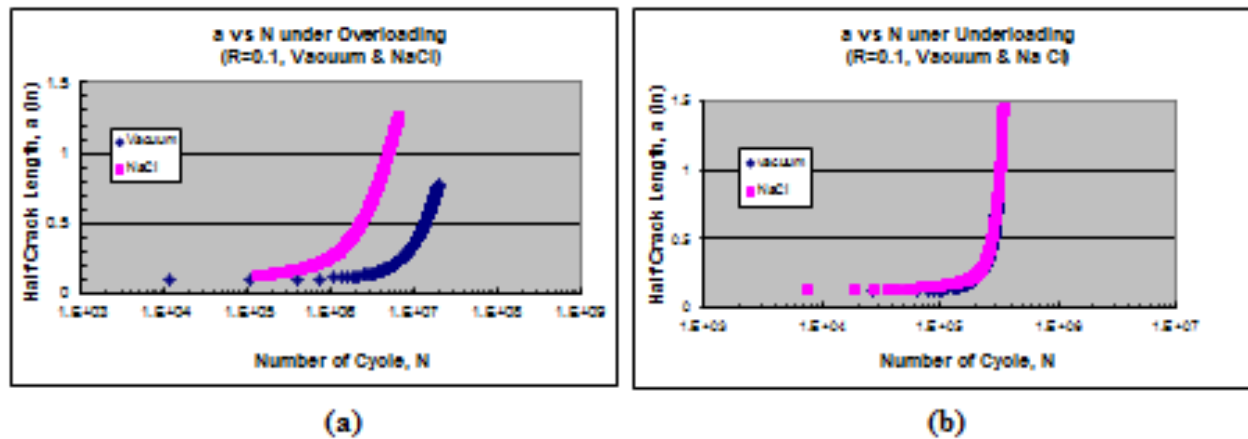


Figure A-6: Variation of Half Crack Length with Number of Loading Cycle at  $R=0.1$  under Overloading and Underloading in Vacuum and 1 Percent NaCl Solution



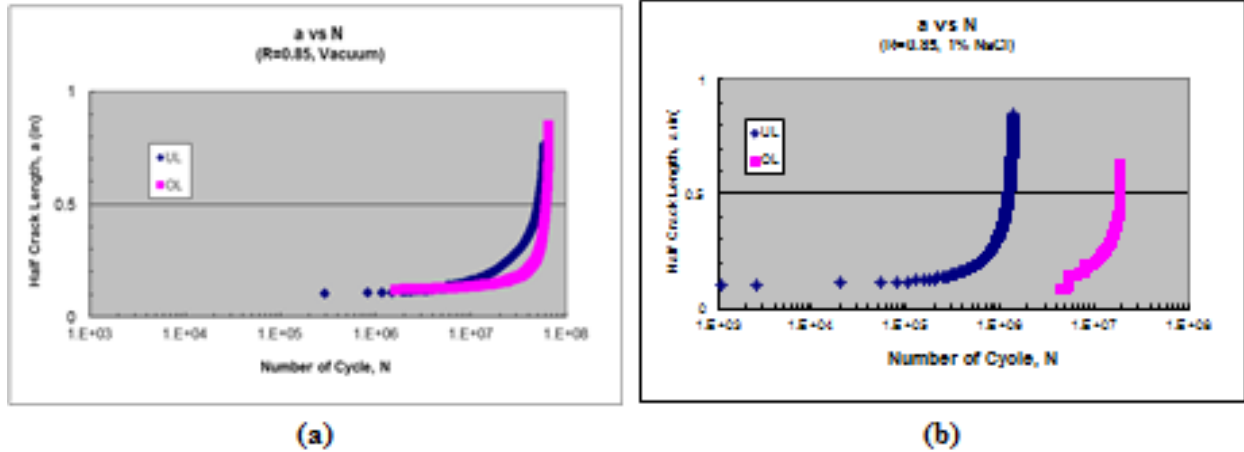


Figure A-7: Variation of Half Crack Length with Number of Loading Cycle at  $R=0.85$  in Vacuum and 1 Percent NaCl Solution under Overloading and Underloading

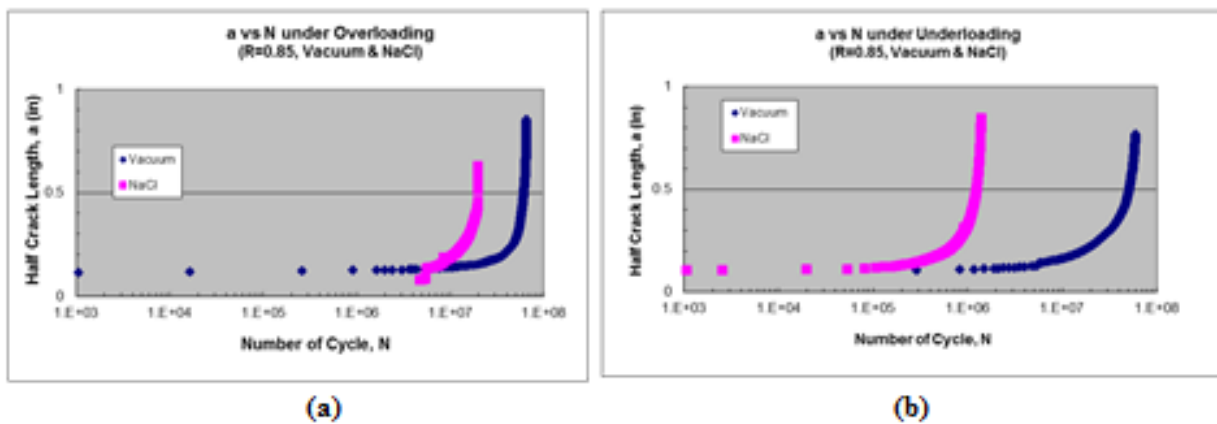


Figure A-8: Variation of Half Crack Length with Number of Loading Cycle under Overloading and Underloading in Vacuum and 1 Percent NaCl Solution

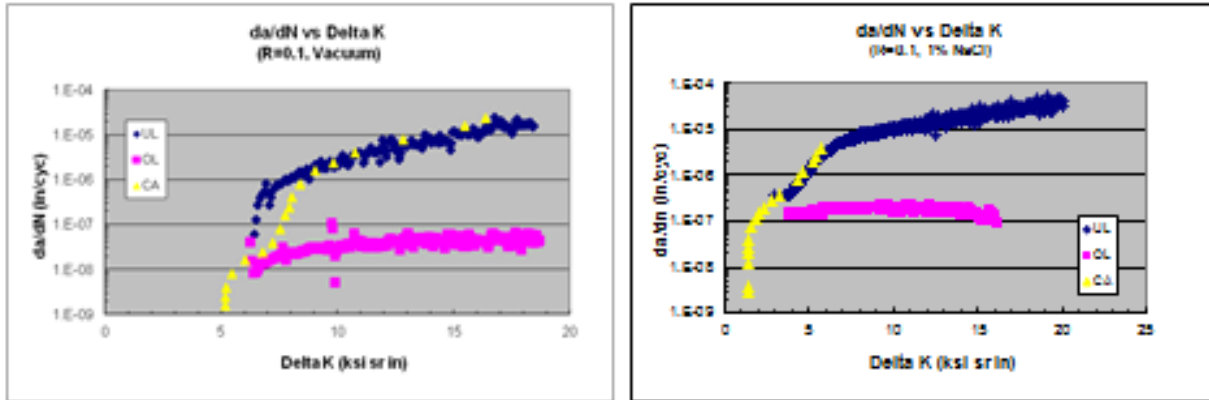


Figure A-9: Effect of Loading on Fatigue Crack Growth Rate at R=0.1 in Vacuum and 1 Percent NaCl Solution

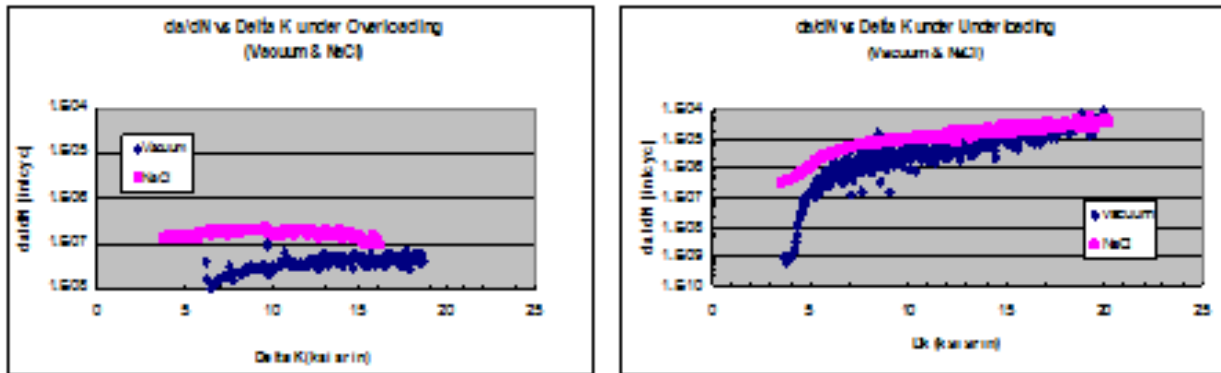


Figure A-10: Effect of Environment on Fatigue Crack Growth Rate at R=0.1 Under Overloading and Underloading

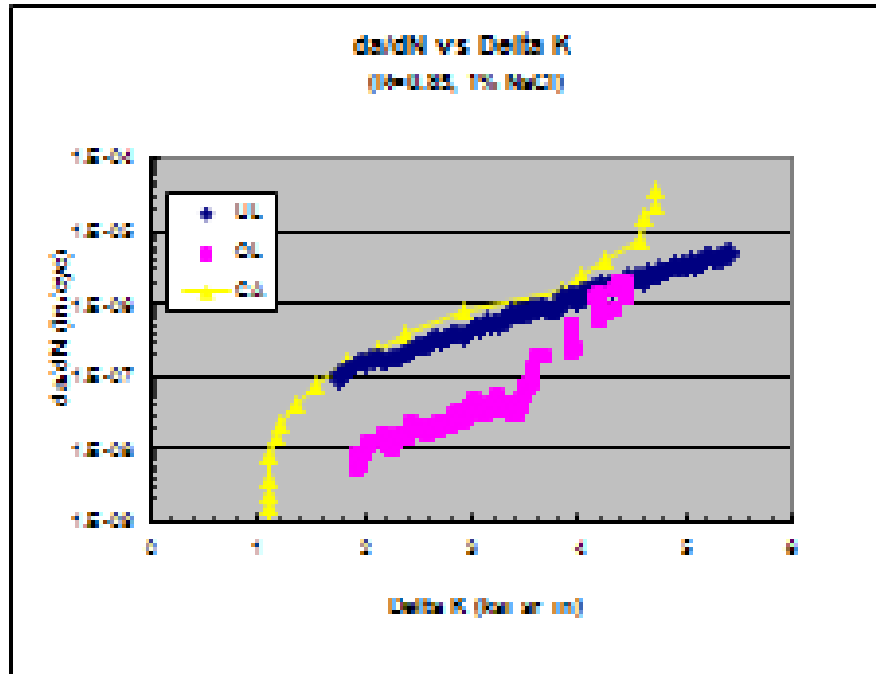


Figure A-11: Effect of Loading on Fatigue Crack Growth Rate at  $R=0.85$  in 1 Percent NaCl Solution

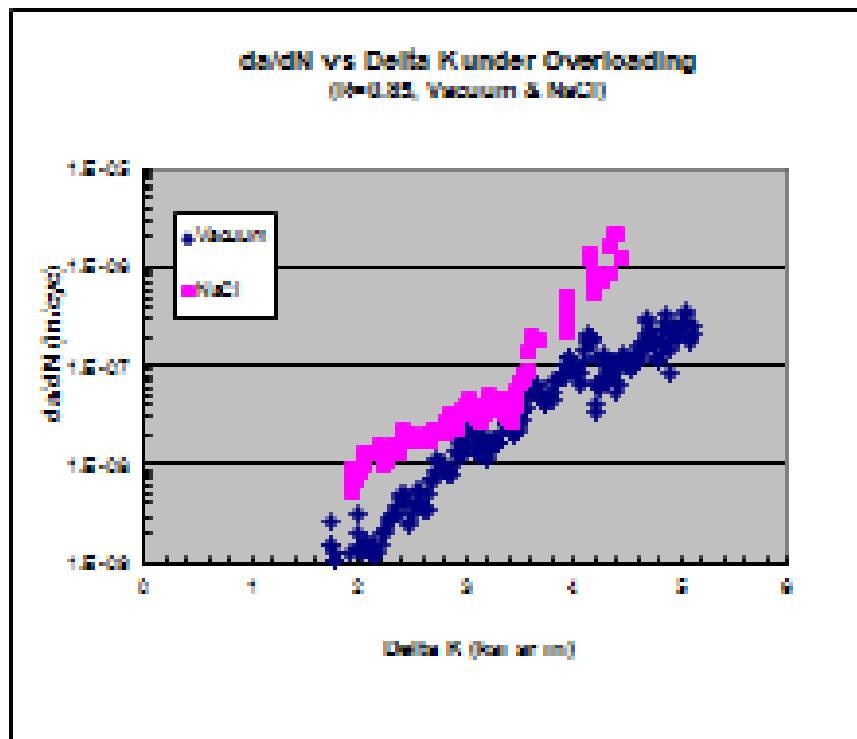


Figure A-12: Effect of Environment on Fatigue Crack Growth Rate at  $R=0.85$  under Overloading

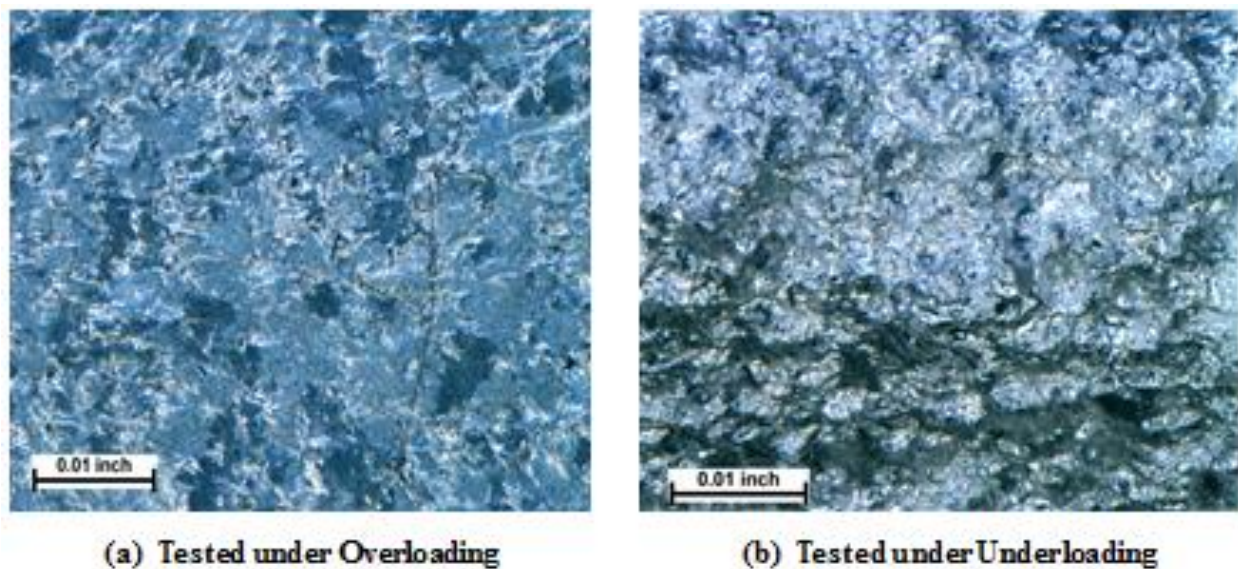


Figure A-13: Optical Fractographs

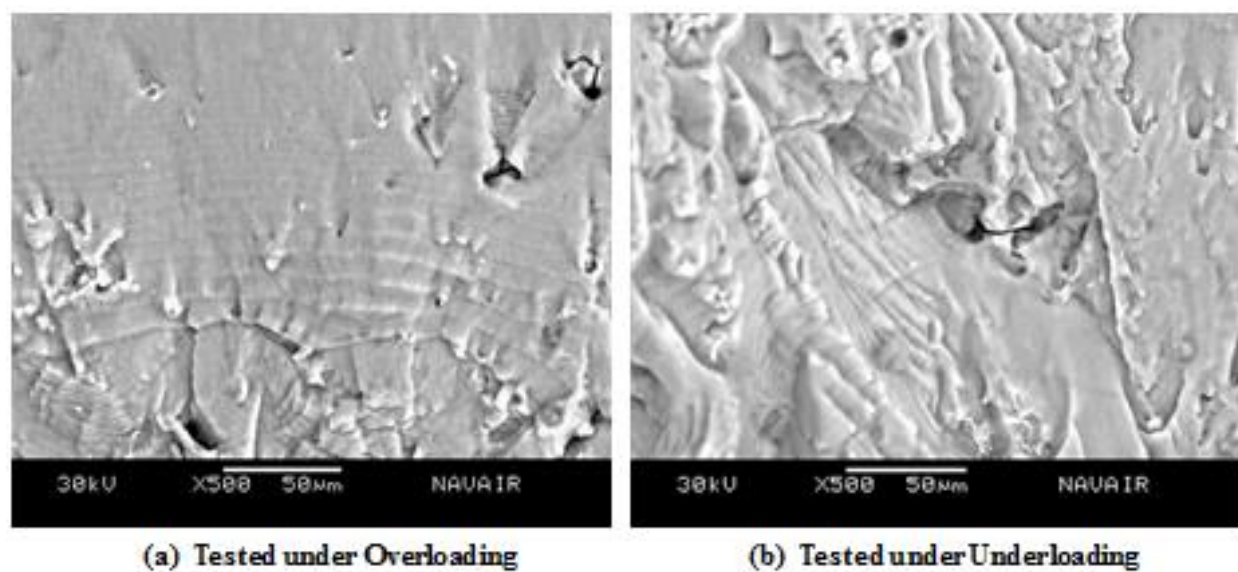


Figure A-14: SEM Fractographs

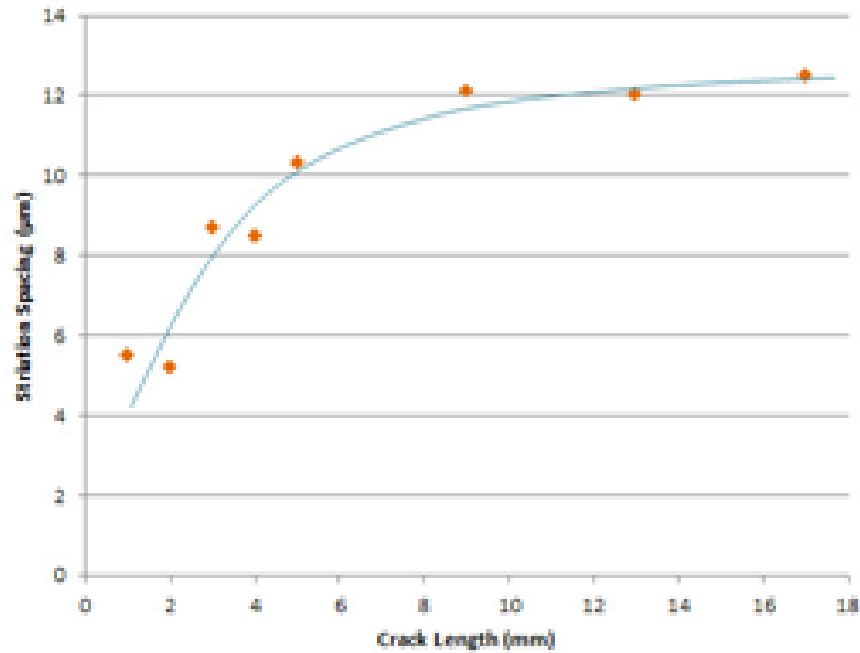


Figure A-15: Variation of Striation Spacing with Crack Length

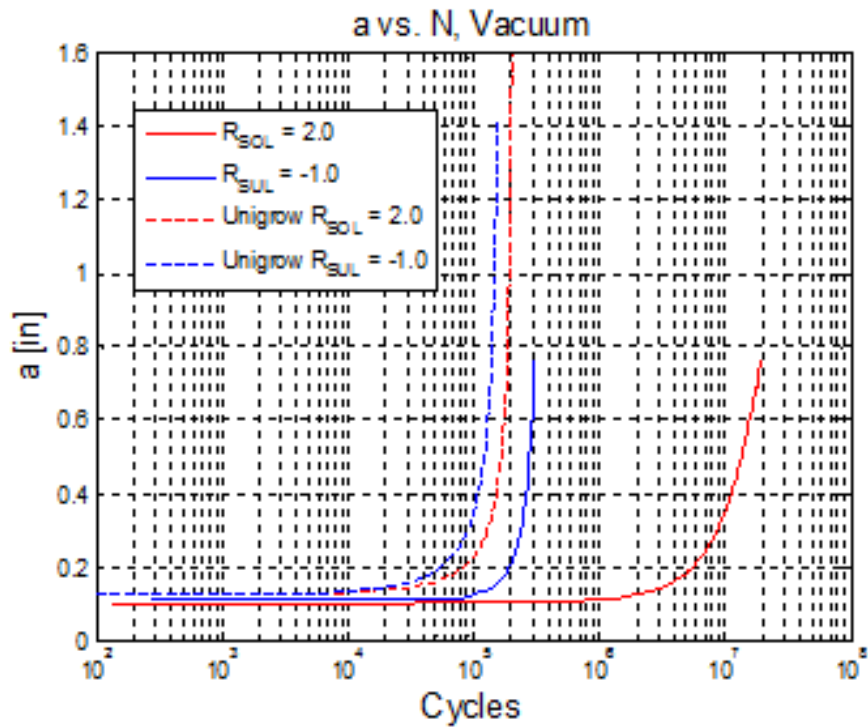
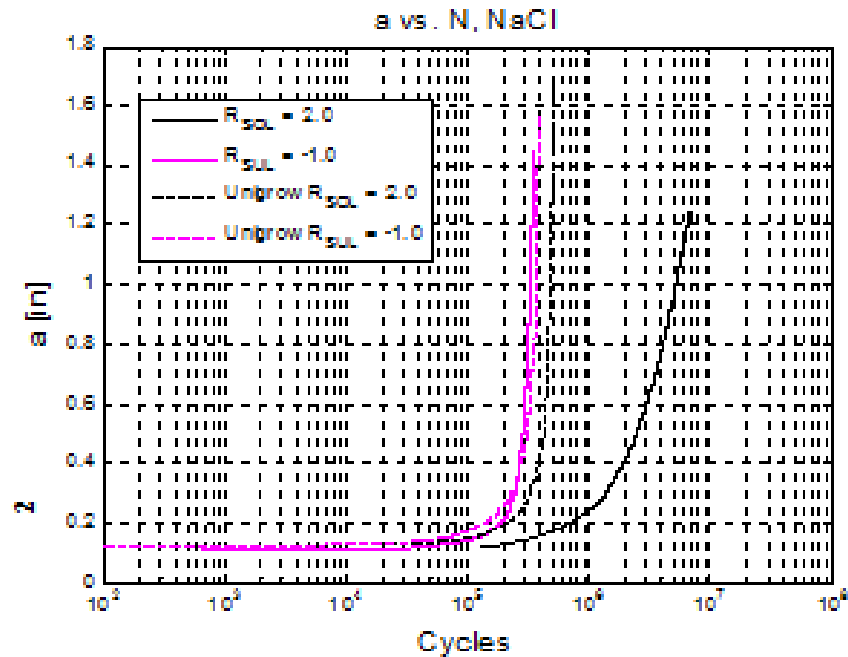


Figure A-16: Graphic Comparison of Test Data and UniGrow Model Prediction for Overload and Underload Spectrums in Vacuum



$R_{SOL} = 2.0$  : Overload Ratio = A 100% OL at Every 10,000 Cycles = Peak OL/Max. Load  
 $R_{SUL} = -1.0$  : Underload Ratio = A 100% UL at Every 10,000 Cycles = Peak UL/Max. Load

Figure A-17: Graphic Comparison of Test Data and UniGrow Model Prediction for Overload and Underload Spectrums in 1 Percent NaCl Solution

DISTRIBUTION:

Office of Naval Research (Code 35/William Nickerson) 875 N. Randolph St., Room 1143B, Arlington, VA 22203	1
NAVAIRSYSCOM (AIR 4.0T/Dr. James Sheehy), Bldg. 2109, Room N122 48150 Shaw Road, Patuxent River, MD 20670	1
NAVAIRSYSCOM (AIR 4.3), Bldg.2187, Suite 3340 48110 Shaw Road, Patuxent River, MD 20670-1906	1
NAVAIRSYSCOM (AIR 4.3T/Jerry Rubinsky), Bldg. 2187, Suite 3322 48110 Shaw Road, Patuxent River, MD 20670-1906	1
NAVAIRSYSCOM (AIR 4.3.4/Darrel Tenney), Bldg. 2188 48066 Shaw Road, Patuxent River, MD 20670-1908	1
NAVAIRSYSCOM (AIR 4.3.4.1/Robert Kowalik), Bldg. 2188 48066 Shaw Road, Patuxent River, MD 20670-1908	1
NAVAIRSYSCOM (AIR 4.3.4.1/Eun U. Lee), Bldg. 2188 48066 Shaw Road, Patuxent River, MD 20670-1908	25
FRC/ISSC Jacksonville (AIR 4.3.4) Naval Air Station, Jacksonville, FL 32212	1
FRC/ISSC Jacksonville (AIR 4.3.4.6/John Benfer) Naval Air Station, Jacksonville, FL 32212	1
NAVAIRWARCENACDIV (4.12.6.2), Bldg. 407, Room 116 22269 Ceder Point Road, Patuxent River, MD 20670-1120	1
DTIC 8725 John J. Kingman Road, Suite 0944, Ft. Belvoir, VA 22060-6218	1

**UNCLASSIFIED**

**UNCLASSIFIED**